Complete discrimination of strain and temperature using Brillouin frequency shift and birefringence in a polarization-maintaining fiber

Weiwen Zou, Zuyuan He, and Kazuo Hotate

Department of Electrical Engineering and Information Systems, The University of Tokyo, 7-3-1 Hongo, Bunkyo-ku, Tokyo 113-8656, Japan
zou@sagnac.t.u-tokyo.ac.jp zhe@ee.t.u-tokyo.ac.jp hotate@sagnac.t.u-tokyo.ac.jp

Abstract: This paper presents a novel method that realizes simultaneous and completely discriminative measurement of strain and temperature using one piece of Panda-type polarization-maintaining fibre. Two independent optical parameters in the fiber, the Brillouin frequency shift and the birefringence, are measured by evaluating the spectrum of stimulated Brillouin scattering (SBS) and that of the dynamic acoustic grating generated in SBS to get two independent responses to strain and temperature. We found that the Brillouin frequency shift and the birefringence have the same signs for strain-dependence but opposite signs for temperature-dependence. In experiment, the birefringence in the PMF is characterized with a precision of ~10^{-8} by detecting the diffraction spectrum of the dynamic acoustic grating. A reproducible accuracy of discriminating strain and temperature as fine as 3 micro-strains and 0.08 degrees Celsius is demonstrated.

OCIS codes: (060.2370) Fiber optics sensors; (290.5900) Scattering, stimulated Brillouin; (120.5820) Scattering measurements; (050.1950) Diffraction gratings.

References and links

1. M. Nikles and L. Thevenaz, "Simple distributed fiber sensor based on Brillouin gain spectrum analysis," Opt. Lett. **21**, 758-760 (1996).
2. D. Garus, T. Gogolla, K. Krebber, and F. Schliep, "Brillouin optical-fiber frequency-domain analysis or distributed temperature and strain measurement," J. Lightwave Technol. **15**, 654-662 (1997).
3. K. Hotate and M. Tanaka, "Distributed fiber Brillouin strain sensing with 1-cm spatial resolution by correlation-cased continuous-wave technique," IEEE Photon. Technol. Lett. **14**, 179-181 (2002).
4. T. Horiguchi, T. Kurashima, and M. Tateda, "Tensile strain dependence of Brillouin frequency shift in silica optical fibers," IEEE Photon. Technol. Lett. **1**, 107-108 (1989).
5. W. Zou, Z. He, and K. Hotate, "Investigation of strain- and temperature-dependences of Brillouin frequency shifts in GeO_2-doped optical fibers," J. Lightwave Technol. **26**, 1854-1861 (2008).
6. C. C. Lee, P. W. Chiang, and S. Chi, "Utilization of a dispersion-shifted fiber for simultaneous measurement of distributed strain and temperature through Brillouin frequency shift," IEEE Photon. Technol. Lett. **13**, 1094-1096 (2001).
7. W. Zou, Z. He, M. Kishi, and K. Hotate, "Stimulated Brillouin scattering and its dependences on temperature and strain in a high-delta optical fiber with F-doped depressed inner cladding," Opt. Lett. **32**, 600-602 (2007).
8. T. P. Parker, M. Farhadiroushan, V. A. Handerek, and A. J. Rogers, "Temperature and strain dependence of the power level and frequency of spontaneous Brillouin scattering in optical fibers," Opt. Lett. **22**, 787-789 (1997).
9. T. Okoshi, "Single-polarization single-mode optical fibers," IEEE J. Quantum Electron. **17**, 879-884 (1981).
10. G. P. Agrawal, *Nonlinear Fiber Optics*, (Academic Press, 3rd version, 2001).
11. W. Zou, Z. He, and K. Hotate, "Two-dimensional finite element modal analysis of Brillouin gain spectra in optical fibers," IEEE Photon. Technol. Lett. **18**, 2487-2489 (2006).
12. K. Y. Song, W. Zou, Z. He, and K. Hotate, "All-optical dynamic grating generation based on Brillouin scattering in polarization-maintaining fiber," Opt. Lett. **33**, 926-929 (2008).

#105264 - $15.00 USD Received 12 Dec 2008; revised 14 Jan 2009; accepted 14 Jan 2009; published 21 Jan 2009

13. X. Bao, Q. Yu, and L. Chen, "Simultaneous strain and temperature measurements with polarization-maintaining fibers and their error analysis by use of a distributed Brillouin loss system," Opt. Lett. **29**, 1342-1344 (2004).
14. S. L. Floch and P. Cambon, "Study of Brillouin gain spectrum in standard single-mode optical fiber at low temperatures (1.4–370 K) and high hydrostatic pressures (1–250 bars)," Opt. Commun. **219**, 395-410 (2003).
15. K. S. Chiang, D. Wong D, and P. L. Chu, "Strain-induced birefringence in a highly birefringent optical fiber," Electron. Lett. **26**, 1344-1346 (1990).

1. Introduction

Brillouin fiber-optic distributed sensors [1-3] have been extensively investigated for two decades and they show great potentials in applications of smart materials and smart structures. So far, Brillouin sensors are categorized by different schemes (i.e., time-domain [1], frequency-domain [2] and correlation-domain [3]) in resolving the sensing location, while their sensing mechanisms are all based on the linear dependences of Brillouin frequency shift (BFS) on strain and/or on temperature [4-5]. This common mechanism results in a heavy trouble for any of above techniques in discriminating the response to strain from that to temperature by using a single piece of fiber. In current practices, two fibers are used to discriminate the strain and the temperature: the first one is embedded or bonded at the target material/structure to feel the total effects of strain and temperature, while the second fiber is placed beside the first one and kept in loose condition so that it feels the effect of temperature only; then the strain and the temperature can be calculated by mathematics. A possible solution using one fiber is to monitor two acoustic resonance peaks at different orders of Brillouin gain spectrum (BGS) in a specially-designed optical fiber [6-7]. So far, this method cannot ensure accurate discrimination because all the acoustic resonance frequencies exhibit similar behaviors in their dependences on strain and temperature [5]. There is also a method reported for the discrimination relying on the possibility that the peak amplitude and BFS in the BGS could have quantitatively different dependences on strain and temperature [8]. Its accuracies is not sufficient either (e.g., several degrees Celsius and hundreds of micro-strains) mainly due to the low signal-to-noise ratio in the BGS peak-amplitude measurement, particularly for distributed sensing where troublesome noise from non-sensing locations is accumulated.

In this paper, we demonstrate a new method for complete discrimination of strain and temperature by use of only one piece of Panda-type polarization-maintaining fiber (PMF). Two independent optical parameters in the fiber, the BFS and the birefringence, are precisely measured to get two independent responses to strain and temperature, from which the strain and the temperature are figured out. The BFS is obtained by monitoring the BGS of stimulated Brillouin scattering (SBS) between pump and probe lightwaves counter-propagating along the fiber, where the pump and probe lightwaves are linearly polarized in one primary axis of the PMF. The birefringence is characterized by detecting the diffraction spectrum of the dynamic acoustic grating generated in SBS with a third lightwave linearly-polarized in the orthogonal primary axis. Experimentally, a discrimination accuracy of 3 με and 0.08 ^{o}C is demonstrated.

2. Principle

The fiber that we employed for discriminative measurement of strain and temperature is a Panda-type PMF, which is composed of two B_2O_3-doped-silica stress-applying parts that are inserted in a pure-silica cladding and symmetrically placed beside a GeO_2-doped-silica core. The fiber sample is only coated with a 250-μm polymer jacket, so that the coating's influence in this study is expected to be negligible. Due to the difference in thermal contraction between B_2O_3-doped silica and pure silica, two-dimensional stress is raised and stored into the core during the drawing process in fiber fabrication [9]. The residual stress makes the refractive index along x-axis (n_x) slightly greater than that along y-axis (n_y). Consequently, a

#105264 - $15.00 USD Received 12 Dec 2008; revised 14 Jan 2009; accepted 14 Jan 2009; published 21 Jan 2009

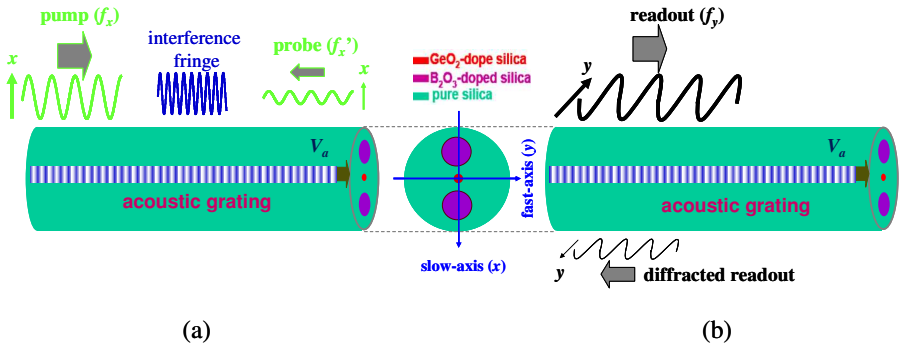

Fig. 1. (a) Strong acoustic grating (phonons) is longitudinally generated by SBS process in a Panda-type polarization-maintaining fiber (birefringence B = ~3.3×10^{-4}) when two linearly-polarized lightwaves (pump and probe) counter-propagate through the fiber with their polarization along the fiber's x-axis (slow axis), and their frequency difference (f_x - f_x') equals the Brillouin frequency shift (ν_B). (b) A linearly-polarized readout light launched into the fiber with its polarization along fiber's y-axis (fast axis) is significantly diffracted backward by the acoustic grating, provided its frequency (f_y) satisfies a birefringence-determined frequency deviation (f_{yx}) from that of pump light.

lightwave linearly polarized along x-axis (so called slow axis) propagates slower than that along y-axis (fast axis). The difference between n_x and n_y (i.e., birefringence $B = n_x - n_y$) is small (e.g., B = ~3.3× 10^{-4} for the fiber used here) but large enough so that lightwaves linearly-polarized along either x- or y-axis can propagate through the fiber while maintaining their polarization states in despite of external disturbance.

The first measurement we perform for the discrimination is the response of BFS to strain and temperature by evaluating the BGS of SBS in the fiber. As schematically shown in Fig. 1(a), two lightwaves, one is called pump with optical frequency f_x and the other called probe with frequency f_x', counter-propagate through the fiber; the pump and the probe are linearly polarized along x-axis, for instance. When the frequency difference between pump and probe f_x - f_x' equals the fiber's acoustic resonance frequency $\nu_B = 2n_x f_x \cdot V_a/c$, where V_a is the acoustic velocity in the fiber and c the light speed in vacuum, SBS occurs in which an acoustic wave (phonons) propagating at velocity V_a is significantly generated. The acoustic wave stretches or compresses the fiber core longitudinally, and thus modulates periodically the refractive index. Consequently, a Bragg grating moving forward at V_a is formed. Such a dynamic acoustic grating diffracts a part of energy of the pump backward, and the diffracted lightwave (Stokes light) experiences the Doppler frequency shift ν_B (also referred to as BFS) [10]. In the fiber, the acoustic velocity V_a is proportional to the axial strain and the temperature on the fiber; therefore, the applied axial strain ($\Delta\varepsilon$) and temperature change ($\Delta T = T_i - 25$; T_i the ambient temperature of the fiber) can be measured as detuning of BFS as

$$\Delta\nu_B = \nu_B - \nu_{B0} = C_\nu^\varepsilon \Delta\varepsilon + C_\nu^T \Delta T \,, \tag{1}$$

where ν_{B0} is the BFS at room temperature (25°C) and in loose condition; C_ν^ε (C_ν^T) is the strain (temperature) coefficient of BFS. Both C_ν^ε and C_ν^T are positive because Young's modulus of silica is nonlinearly increased by either $\Delta\varepsilon$ or ΔT [5].

Secondly, we measure the effect on the fiber's birefringence from the applied strain ($\Delta\varepsilon$) and temperature variation (ΔT) by characterizing the dynamic acoustic grating in SBS with a y-polarized lightwave (readout light) launched into the fiber from the same end as the pump [see Fig. 1(b)]. We have demonstrated recently that, because the acoustic wave as a longitudinal wave exhibits no dependence on transverse polarization [11], the y-polarized readout light can also be strongly diffracted by the acoustic grating generated by x-polarized pump and probe, as long as the frequency f_y of the y-polarized readout light satisfies a phase

#105264 - $15.00 USD Received 12 Dec 2008; revised 14 Jan 2009; accepted 14 Jan 2009; published 21 Jan 2009

matching condition that requires f_y to deviate from that of the x-polarized pump (f_x) by a birefringence-determined frequency deviation ($f_{yx} = f_y - f_x = f_x \cdot B/n_x$) [12]. The birefringence B, on the other hand, has linear dependence on axial strain ($\Delta\varepsilon$) and temperature variation (ΔT). Therefore, we get a second measure of the response to $\Delta\varepsilon$ and ΔT by evaluating the variation in the frequency deviation f_{yx} as

$$\Delta f_{yx} = f_{yx} - f_{yx0} = C_f^{\varepsilon}\Delta\varepsilon + C_f^{T}\Delta T\,, \tag{2}$$

where f_{yx0} is the frequency deviation at 25°C and in loose condition; C_f^{ε} and C_f^{T} are the strain coefficient and the temperature coefficient of the frequency deviation, respectively. It is proved that the strain coefficient C_f^{ε} is positive while the temperature coefficient C_f^{T} is negative (see details in Appendix), which means that the responses of the birefringence-determined frequency deviation to strain and to temperature are in opposite directions.

By solving equations (1) and (2) jointly, we get the strain ($\Delta\varepsilon$) and temperature (ΔT) as

$$\begin{pmatrix}\Delta\varepsilon\\ \Delta T\end{pmatrix} = \frac{1}{C_\nu^{\varepsilon}\cdot C_f^{T} - C_\nu^{T}\cdot C_f^{\varepsilon}}\begin{pmatrix}C_f^{T} & -C_\nu^{T}\\ -C_f^{\varepsilon} & C_\nu^{\varepsilon}\end{pmatrix}\begin{pmatrix}\Delta\nu_B\\ \Delta f_{yx}\end{pmatrix}, \tag{3}$$

Because C_f^{T} has a sign opposite to those of other three coefficients, the denominator ($C_\nu^{\varepsilon}\cdot C_f^{T}$ - $C_\nu^{T}\cdot C_f^{\varepsilon}$) of equation (3) has significant value, i.e., equations (1) and (2) are independent to each other, ensuring high discrimination accuracy. In experiment described later, we demonstrated an accuracy of 3 $\mu\varepsilon$ for strain and 0.08 °C for temperature. This result reflects the fact that the two physical phenomena/quantities that we utilize for the discrimination, the BFS and the birefringence of the fiber, are inherently independent.

3. Experimental details

Experimental demonstration on our novel method was performed with a setup shown in Fig. 2. Part A in Fig. 2 is a typical pump-probe scheme to measure BGS (and thus BFS ν_B) [7], except that a set of polarization-maintaining (PM) components (polarizer, PM isolator, PM

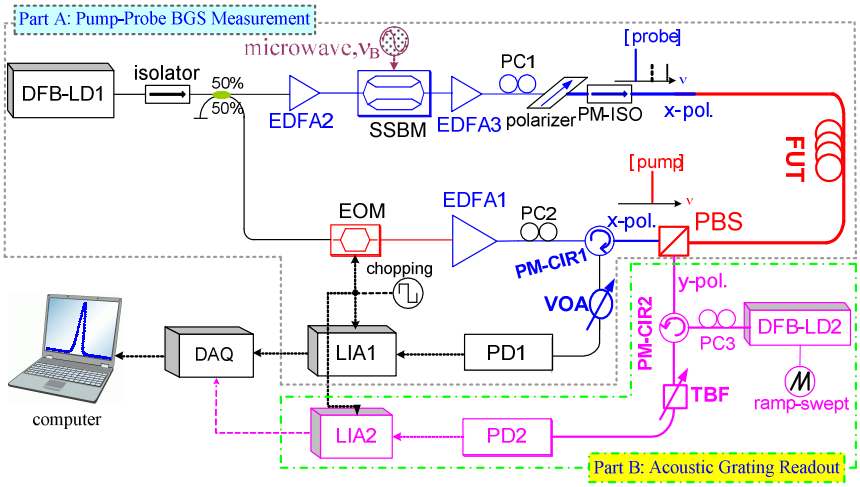

Fig. 2. Configuration of the measurement system. Part A, Pump-probe scheme to measure the Brillouin gain spectrum and thus the Brillouin frequency shift along x-axis. Part B, Detection of the diffraction spectrum of the acoustic grating in SBS to y-polarized readout light. DFB-LDs, distributed-feedback laser diodes; EDFAs, erbium-doped fiber amplifiers; SSBM, single-sideband electro-optic modulator; EOM, intensity electro-optic modulator; PCs, polarization controllers; VOA, variable optical attenuator; TBF, tunable band-pass filter; PDs, photo-diodes; LIAs, lock-in amplifiers; DAQ, data acquisition card; FUT, fiber sample under test; PM, polarization-maintaining; PM-CIRs, PM circulators; PM-ISO, PM isolator; PBS, polarization beam splitter/combiner.

#105264 - $15.00 USD Received 12 Dec 2008; revised 14 Jan 2009; accepted 14 Jan 2009; published 21 Jan 2009

circulator, and polarization beam splitter/combiner) are introduced to ensure the pump and probe lightwaves polarized along *x*-axis. The light source is a 1,549-nm distributed-feedback laser diodes (DFB-LD1). The intensities of the pump and the probe incident to a 31-meter long fiber under test (FUT) are amplified with erbium-doped fiber amplifiers to ~140 mW and ~1 mW, respectively. The frequency of the probe is down-shifted from that of the pump for 10.8 GHz to 11.1 GHz with a single-sideband electro-optic modulator controlled by a microwave synthesizer, so the BGS is obtained as shown in Fig. 3(a), which depicts the BGS of the 31-meter FUT. Synchronous detection scheme was employed by chopping the pump with electro-optic modulator (EOM) and detecting with a lock-in amplifier (LIA1) to ensure high precision in characterization of BFS ν_B. A reproducible accuracy of 0.1 MHz was confirmed [7].

Part B in Fig. 2 is for measuring the diffraction spectrum of the dynamic acoustic grating to *y*-polarized readout light (and thus the birefringence-determined frequency deviation f_{yx}). The readout light is generated from the other laser diode DFB-LD2 (central wavelength ~1,549 nm), whose optical frequency is ramp-swept by linearly modulating its dc injection current. Through the polarization beam splitter/combiner after a PM circulator, the linearly polarized readout light (intensity ~63 mW) is launched into the FUT with its polarization along the fiber's *y*-axis. At first, the acoustic phonons in SBS (and thus the dynamic acoustic grating) are maximized by fixing the microwave frequency to the single-sideband modulator at the BFS ν_B obtained above. Under this condition, the readout light is strongly diffracted by the acoustic grating. The diffracted light is detected synchronously by using the other lock-in amplifier (LIA2) and recorded as a function of the ramp-swept optical frequency of DFB-LD2. In this way, the diffraction spectrum of the acoustic grating to *y*-polarized readout light is obtained. For measuring the diffraction spectrum, a tunable optical band-pass filter with ~20-GHz bandwidth is used to eliminate the leakage of *x*-polarized probe and pump. The diffraction spectrum of the dynamic acoustic grating established over the 31-meter FUT measured at room temperature is plotted in Fig. 3(b). Figure 3(b) shows that the diffraction spectrum has a profile Gaussian-like rather than Lorentzian. By least-squares Gaussian fitting to the experimental data in Fig. 3(b), we get the birefringence-determined frequency deviation f_{yx} = 43.8765 GHz representing the fiber's birefringence $B = 3.27773 \times 10^{-4}$, and the FWHM (full width at the half magnitude) as ~320 MHz. It is not clear why the diffraction spectrum is Gaussian-like and the width of the diffraction spectrum is quite larger than the Brillouin linewdith. Further research is needed on this point. Repeatability test result validates that the frequency deviation can be measured within a standard error of δf_{yx} = 4 MHz corresponding to a reproducible $\delta B = 3 \times 10^{-8}$. The accuracy is fine enough to characterize the birefringence's dependence on strain and temperature as described below. Comparatively, a published method

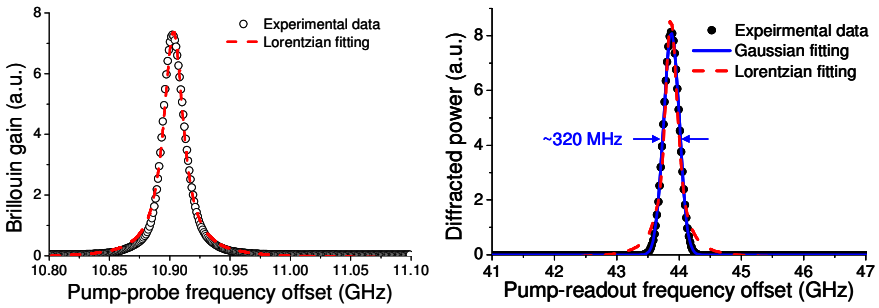

Fig. 3. Measured Brillouin gain spectrum (a) and the diffraction spectrum of the dynamic acoustic grating induced by SBS to *y*-polarized readout light (b) in a 31-meter-long fiber at room temperature and in loose condition. Circles denote experimental data. The solid (dashed) curve corresponds to Gaussian (Lorentzian) fitting to experimental data.

#105264 - $15.00 USD Received 12 Dec 2008; revised 14 Jan 2009; accepted 14 Jan 2009; published 21 Jan 2009

based on simply switching the SBS measurement along *x*-axis and *y*-axis [13] can only give birefringence accuracy around 10^{-5}, which is insufficient for characterizing strain and temperature responses of the birefringence and for strain and temperature discrimination.

The BGS and the diffraction spectrum were measured when different strains were applied upon the 31-meter FUT. The fiber was hand-wound around a couple of drums for tens of circles that were inserted into a temperature-controlled water bath and mounted on *x*-stages for applying strain [7]. The applied strain was evaluated as the ratio of the displacement of the movable *x*-stage to the half-circle segment fiber length. The temperature of the water bath can be controlled with 0.1-^{o}C accuracy. The measurement results are shown in Fig. 4(a) and 4(c). As the applied strain increases, both the BGS and the diffraction spectrum move towards a higher frequency. It is noticed that both spectra broaden while their peak amplitudes decrease as the applied strain increasing. This is because each circle of fiber segment possesses slightly different zero-strain initial condition so that more or less position-dependent stretched strain along the fiber is introduced. As the result, the measured spectra that are the integral over the whole-length fiber become broadened, and the peak amplitudes that are inversely proportional to the width of the spectra [10] reduce.

Next, we investigated the influence of the fiber's temperature on the BGS and the diffraction spectrum of the dynamic grating to *y*-polarized readout light. Figures 4(b) and 4(d) illustrate the BGS and the diffraction spectra, respectively, with respect to temperature. It is shown of great interest that the BFS ν_B moves towards a higher frequency whereas the frequency deviation f_{yx} shifts to a lower frequency as the temperature increases. The figures also show that both spectra's widths decrease but their peak amplitudes increase with temperature. The increased peak amplitudes are due to the reduced acoustic loss with

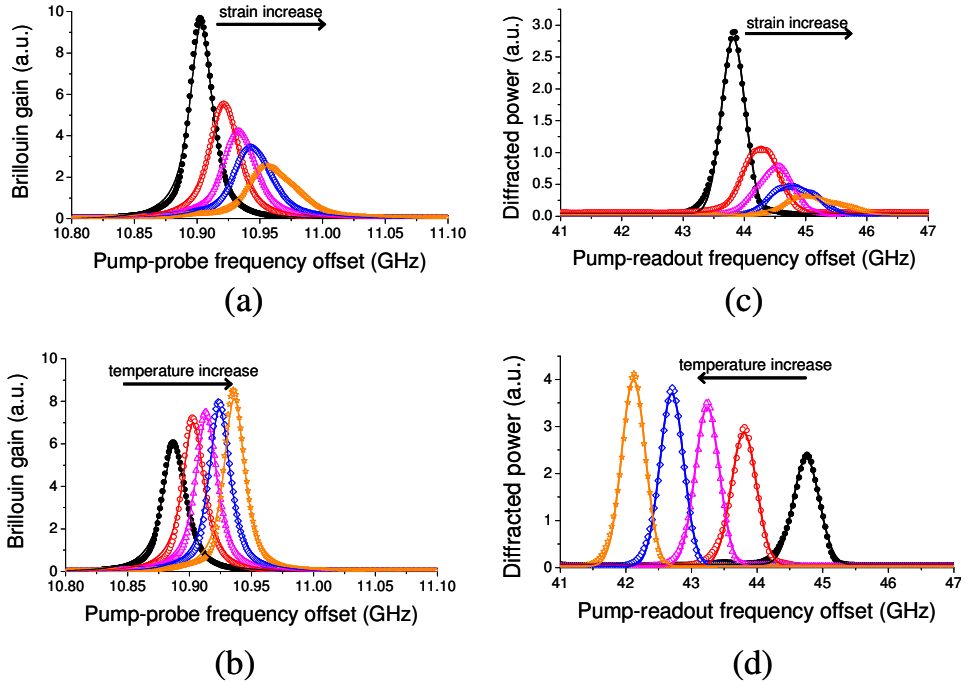

Fig. 4. Dependences of the spectra on strain and temperature. Measured Brillouin gain spectra when applied strain is enlarged (a) or temperature is increased (b). Measured diffraction spectra of the acoustic grating with an incremental strain (c) or temperature (d). Symbolic points, experimental data. Solid curves denotes Lorentzian fitting in (a) and (b) or Gaussian fitting in (c) and (d) giving Brillouin frequency shift (ν_B) or the birefringence-determined frequency deviation (f_{yx}), respectively.

#105264 - $15.00 USD Received 12 Dec 2008; revised 14 Jan 2009; accepted 14 Jan 2009; published 21 Jan 2009

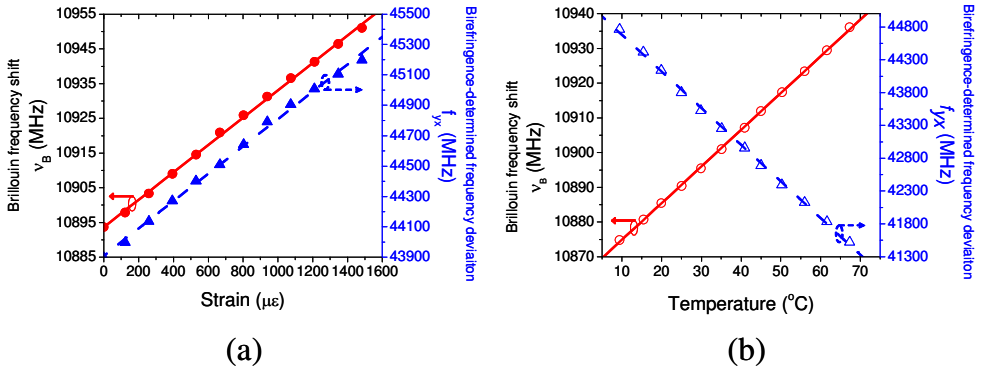

Fig. 5. Measured strain and temperature coefficients. (a) Strain dependence. (b) Temperature dependence. Circles denote the experimental results for Brillouin frequency shift (ν_B) in left vertical axes, and triangles correspond to the birefringence-determined frequency deviation (f_{yx}) in right vertical axes, respectively.

increased temperature. Taken into account the fact that the electrostrictive coefficient is mostly temperature-independent [14], the widths inversely proportional to the peak amplitudes [10] decrease with increased temperature.

The measurement results of strain and temperature dependences of the BFS ν_B and the frequency deviation f_{yx}, which are obtained by Lorentzian fitting to the BGS and Gaussian fitting to the diffraction spectra, respectively, are summarized in Fig. 5. It demonstrates that for the strain variation, the BFS ν_B and the frequency deviation f_{yx} behave similarly; while for the temperature change, they react in opposite direction. All the dependences show excellent linearity; thus by linear fitting, we get the strain coefficient and the temperature coefficient of C_ν^ε = +0.03938 MHz/με and C_ν^T = +1.0580 MHz/°C for the BFS ν_B, and C_f^ε = +0.8995 MHz/με and C_f^T = -55.8134 MHz/ °C for the frequency deviation f_{yx}, respectively. Especially, the coefficients for the frequency deviation f_{yx} match well with our theoretical estimations (see Appendix).

Putting above strain/temperature coefficients into Eq. (3), and taking the standard errors of our measurement system ($\delta\nu_B = 0.1$ MHz and $\delta f_{yx} = 4$ MHz, respectively) into account, the accuracy of the discrimination is given as high as $\delta\varepsilon = \pm 3.1$ με and $\delta T = \pm 0.078$ °C. This high accuracy proves the ability of completely discriminative sensing of strain and temperature. When a set of strain and temperature ($\Delta\varepsilon$, ΔT) was initialized as (0 με, 4.9 °C) or (939 με, 0 °C) in Fig. 5, for example, two frequency changes ($\Delta\nu_B$ and Δf_{yx}) were measured as (5.1 MHz, -276 MHz) or (37.1 MHz, 849 MHz). According to Eq. (3), the strain and the temperature values are calculated as (-2.3με, 4.907°C) or (942.6 με, -0.0197 °C), respectively. They differ from the initialized values with errors as low as (-2.3 με, 0.007 °C) or (3.6 με, -0.020 °C). This example also verifies the complete discrimination ability of our proposed method.

4. Conclusion

We have theoretically and experimentally demonstrated that the BFS (ν_B) and the birefringence-determined frequency deviation (f_{yx}) in a Panda-type PMF have independent responses to strain and temperature. Two independent parameters (ν_B and f_{yx}) have the same signs of strain dependence but the opposite signs of temperature dependence. We proposed to utilize the characteristics as a novel technique to discriminate the response to strain from that to temperature. Simultaneous measurements of the BFS and the birefringence-induced frequency deviation provide a high reproducible accuracy of 3 με and 0.08 °C.

#105264 - $15.00 USD Received 12 Dec 2008; revised 14 Jan 2009; accepted 14 Jan 2009; published 21 Jan 2009

Appendix

The residual tensile stress (σ_{xy}) determining the Panda-type PMF's birefringence scales with the ambient temperature (T_i):

$$B \propto \sigma_{xy} = k \cdot (\alpha_3 - \alpha_2) \cdot (T_{fic} - T_i), \tag{A1}$$

where T_{fic} denotes the fictive temperature (e.g., 850 ^{o}C) of silica glass, α_3 (α_2) the thermal coefficient of B_2O_3-doped-silica stress-applying parts (pure-silica cladding), and k a constant determined by the geometrical location of stress-applying parts in the fiber [15]. When temperature increases ($\Delta T = T_i - 25 > 0$), the residual stress is released and thus the birefringence decreases as

$$\Delta B^T = -B_0 \cdot \frac{\Delta T}{T_{fic} - 25}, \tag{A2}$$

where B_0 is the intrinsic birefringence at room temperature (T_i = 25 ^{o}C). In contrast, when an axial strain $\Delta\varepsilon$ is applied upon the fiber, additional stress is generated because the stress-applying parts and the cladding contract in the lateral direction differently due to their different Poisson's ratios ($\gamma_3 > \gamma_2$) [15], the birefringence is enlarged with applied strain as

$$\Delta B^{\varepsilon} = +B_0 \cdot \frac{(\gamma_3 - \gamma_2)}{(\alpha_3 - \alpha_2)(T_{fic} - 25)} \cdot \Delta\varepsilon, \tag{A3}$$

Consequently, the birefringence-determined frequency deviation f_{yx} varies linearly with respect to temperature increase and to applied strain but in opposite directions as described in Eq. (2), i.e., $\Delta f_{yx} = C_f^{\varepsilon} \cdot \Delta\varepsilon + C_f^{T} \cdot \Delta T$, where the strain coefficient

$$C_f^{\varepsilon} = +f_{yx0} \cdot \frac{(\gamma_3 - \gamma_2)}{(\alpha_3 - \alpha_2)(T_{fic} - 25)}, \tag{A4}$$

and temperature coefficient

$$C_f^{T} = -f_{yx0} \cdot \frac{1}{(T_{fic} - 25)}, \tag{A5}$$

Using our measured result f_{yx0} = 43.875 GHz [see Fig. 3(b)] together with Chiang *et al.*'s result [15] of $(\gamma_3 - \gamma_2)/[(\alpha_3 - \alpha_2)(T_{fic} - 25)] = 24.3\times10^{-6}$ $\mu\varepsilon^{-1}$, the coefficients in the fiber are deduced approximately to be C_f^{ε} = +1.069 MHz/με and C_f^{T} = -54.8 MHz/^{o}C, respectively.

Acknowledgments

This work was supported by the "Grant-in-Aid for Creative Scientific Research" and the "Global Center of Excellence Program (G-COE)" from the Ministry of Education, Culture, Sports, Science and Technology, Japan. Prof. K. Y. Song at Chung-Ang University, Korea, is acknowledged for discussions in the experiment.

#105264 - $15.00 USD Received 12 Dec 2008; revised 14 Jan 2009; accepted 14 Jan 2009; published 21 Jan 2009